Integration of laser scanning and thermal imaging in monitoring optimization and assessment of rockfall hazard: a case history in the Carnic Alps (Northeastern Italy)

Giordano Teza · Gianluca Marcato · Alessandro Pasuto · Antonio Galgaro

Abstract Rock cliff monitoring to evaluate related rockfall hazard requires a deep knowledge of the geometry and kinematics of the rock mass and a real-time survey of some key features. If a sedimentary rock system has sloping discontinuity planes, an open joint could become a potential sliding surface and its conditions must be monitored. It is the case of the Passo della Morte landslide (Carnic Alps, Northeastern Italy), where sub-vertical joints exist. Remote sensing techniques such as terrestrial laser scanning (TLS) and infrared thermography (IRT) allow a fast and efficient contactless geometrical and geomechanical examination of a rock mass. Therefore, they can be used to recognize those joints that require monitoring with on-site instrumentation such as extensometers and/or inclinometers, or also acoustic emission sensors, aiding the arrangement of monitoring systems which are generally quite expensive to install. Repeated IRT surveys would provide useful information about the evolution of unstable slopes, thus suggesting how the on-site monitoring system could be improved. Moreover, data gathered by TLS and IRT can be directly used in landslide hazard assessment. In the test site, an open joint was recognized together with a fair joint that could change in the next future. The results were validated by means of extensometer data.

Keywords Rock slope instability · Rockfall · Thermal imaging · Laser scanning · Monitoring

1 Introduction

Assessment and mitigation of hazard induced by rock slope instability is a very important topic, particularly where there is a threat to life or property. Regardless of the size of the

G. Teza (✉) · A. Galgaro
Dipartimento di Geoscienze, Università di Padova, Via Gradenigo 6, 35131 Padua, Italy
e-mail: giordano.teza@unipd.it

G. Marcato · A. Pasuto
Consiglio Nazionale delle Ricerche, IRPI, Corso Stati Uniti, 4, 35127 Padua, Italy

phenomenon, a landslide affecting a rock slope generally speeds up in its later stages, with a relatively sudden fall of the material (Corominas et al. 2005; Budetta 2010).

Besides classical geological and geomechanical surveys, nowadays several monitoring techniques are used to provide information on the conditions of a rock mass. The geometry and kinematics of an unstable slope can be assessed remotely by terrestrial laser scanning (TLS) (Teza et al. 2008; Oppikofer et al. 2009), digital photogrammetry (Sturzenegger and Stead 2009) and interferometric radar (Singhroy and Molch 2004). Moreover, the TLS can be used to perform a contactless geomechanical survey (Slob et al. 2005) as well as to detect different types of lithology (Franceschi et al. 2009). Ground-penetrating radar (Deparis et al. 2007) and infrared thermography (IRT) (Wu et al. 2005; Teza et al. 2012) can be used to evaluate the conditions of the shallower part of a rock mass, and active and passive seismic methods make it possible to examine the deeper layers of the observed rock mass (see, e.g., Hack 2000). Also, local seismicity can be used to provide information about the precursory fractures of a large and destructive rockfall event (Dixon and Spriggs 2007; Walter et al. 2012).

Conventional instrumentation like extensometers and inclinometers are currently used in landslide monitoring with good results (Corominas et al. 2000). However, these techniques require relatively expensive installation procedures in potentially dangerous locations. Therefore, sensors capable of detecting precursory rockfall signals need to be well placed to maximize their detection of significant indicators of landslide displacements. Microtremors (MTs) and acoustic emissions (AEs) caused by rock fracturing are rockfall precursory signals (Cai et al. 2007; Arosio et al. 2009). They are elastic waves in the sonic band, i.e., frequency below 20 kHz, and in ultrasonic band, 20–50 kHz, for MT and AE, respectively.

This paper shows the results of TLS- and IRT-based measurements on an unstable sedimentary rock mass (Passo della Morte Landslide, Carnic Alps) continuously monitored by means of extensometers, inclinometers and AE sensors. The research aims to evaluate the role that TLS and IRT can play in optimization of on-site sensor location and to acquire information on the way the unstable slope behaves.

2 The Passo della Morte landslide

2.1 Geological setting

The Passo della Morte landslide (Ampezzo and Forni di Sotto Municipalities, Udine Province, Friuli Venezia Giulia Region) is a very large landslide in the Carnic Alps, affecting slopes on the left bank of the Tagliamento River (Fig. 1). Several hillslope processes exist in this area, with different typologies and current states of activity, and are mainly related to debuttressing induced by the melting of a glacier that occupied the valley until approximately 10,000 years ago (Pisa 1972; Marcato 2007; Monegato and Vezzoli 2011).

In the western part of this physical context, there is a cliff whose geological setting makes it particularly prone to instability (Fig. 2a). This paper focuses on this area only, which has limestone (dark-layered limestone—Lower Carnian), with dolomite (Dolomia dello Schlern—Upper Ladinian) as the underlying bedrock. It is characterized by sub-vertical layers with open joints. The rock mass is approximately 130 m wide and 250 m high, from 650 to 900 m above sea level (a.s.l.). It is densely stratified, with layers of variable thickness, but rarely more than 0.5 m thick. Sometimes, the limestone alternates
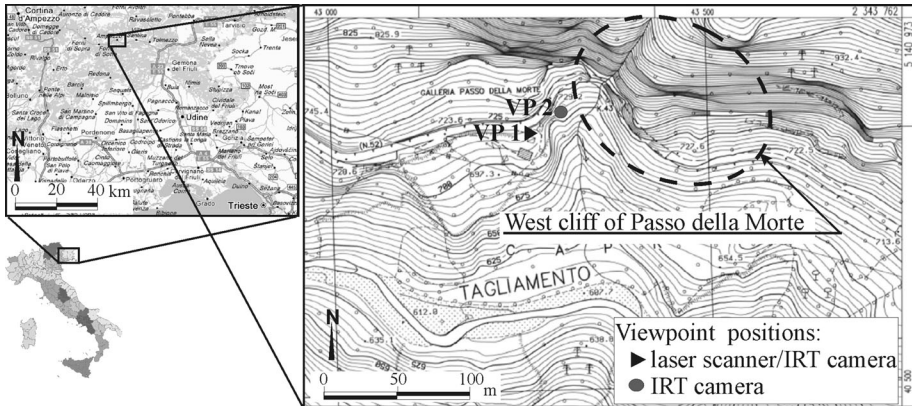
Fig. 1 Localization of Passo della Morte landslide, whose western part is studied here. Laser scanner and IR thermography viewpoints are highlighted

Fig. 2 Monitoring systems: **a** view of west rock cliff and extensometer positions (EXT4–EXT6), where borders between dolomite bedrock and limestone (*dashed line*) and between zone A and zone B (*dotted line*) are shown; **b** plan view of rock mass and monitoring system layout, where all extensometers (EXT1–EXT6), seismic station (MORT), acoustic emission waveguides (AEWG 1, 2) and location of inclinometer tube borehole (BH) are shown. Dip and dip direction of the bedding plane are also reported. Finally, CVP is the location of the camera viewpoint used to take the image in (**a**)
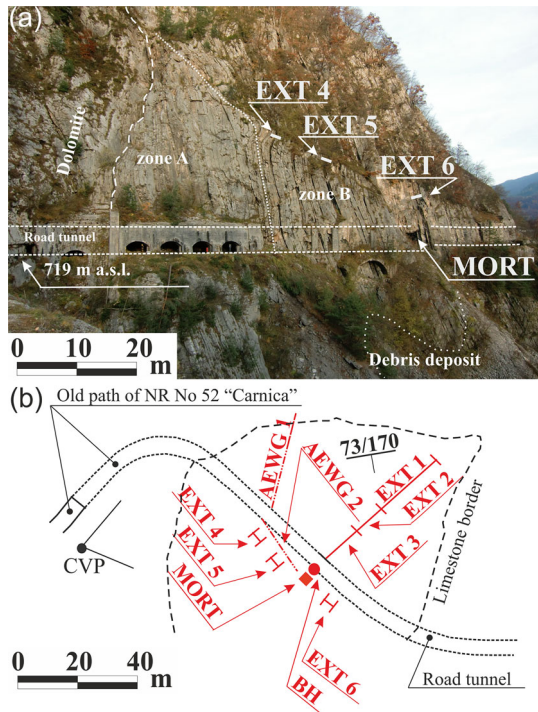
with marl, more or less calcareous, of varying thickness, from a few millimeters to 0.25 m. The dip direction of the layers coincides with the slope, with layers inclined at 73° toward the river. Since the strata present a sub-vertical attitude, open joints, several centimeters in width, exist and these conditions easily allow infiltration of water into the rock mass when it rains, thus favoring slope failures. Two distinct zones can be recognized in the limestone rock mass (Fig. 2a): zone A, which is characterized by planar and slightly irregular beds

and where the joints are substantially closed or, rarely, a few millimeters open without fill material, and zone B, characterized by planar or undulating discontinuities that in some cases are open, or partially open, often having marl in-filling.

The instability is related to both single rockfall events involving blocks of ~ 1 m^3 and sliding processes that could affect a significant part of the limestone rock mass (Codeglia 2011). In particular, there are two possible sliding failure processes involving the stratified system and controlled by the limestone bedding and orthogonal joint system; the first one should be related to the weak contact between A and B zones (involved rock volume: $\sim 450,000$ m^3) and the second one could be related to the contact between dolomite and limestone (involved volume: $\sim 700,000$ m^3). Since it seems that the hazard is mainly related to zone B, a contactless identification of the border between these zones is one of the aims of the present study. More information about the phenomenon can be found in Marcato (2007), and a discussion of the possible evolutionary scenarios of the landslide can be found in Dixon et al. (2012).

The landslide directly threatened the National Road no. 52 "Carnica." For this reason, the path of road was recently changed. The old route, with a 200-m-long tunnel passing through the dark-layered limestone rock mass, was replaced in 2007 by a new 2-km-long tunnel. Since the phenomenon has a potential impact on the Tagliamento River through valley damming, the induced risk is considered high (Figs. 1, 2).

The Passo della Morte area is characterized by a significant level of seismicity. Therefore, a seismic station (called MORT) belonging to the Friuli Venezia Giulia seismic monitoring network (OGS 2014) was placed within the old road tunnel. This station monitors both earthquake events and landslide-induced MTs in the range 0.1–100 Hz.

Several geophysical surveys were carried in the recent past, including ground-penetrating radar and active and passive seismic surveys (Dixon et al. 2012). Two seismo-stratigraphic units were recognized: first, shallower unit characterized by a thick layer (from 8 to 15 m) of limestone and second deeper unit.

2.2 Monitoring activities

Three high-accuracy extensometers (EXT4, EXT5 and EXT6) were placed in 2010 in zone B, where open joints were observed by means of geomorphological and geostructural survey. Since the instability processes are more probably along the bedding planes, each extensometer intersects a possible sliding feature (the joint families are described in detail in Chapter 3). Figure 2 shows the extensometer positions, the corresponding monitored joints and a map of the monitoring systems, including a 100-m-long inclinometric tube placed in a drilled borehole.

The extensometer EXT4 recorded subcentimetric/centimetric displacements, whereas EXT5 and EXT6 did not measure any significant deformation, i.e., the measurements were below the instrument's accuracy threshold (Table 1). Moreover, the displacements measured by EXT4 in 2012 and 2013 were higher than those detected in 2011 (9.1 and 12.5 mm/year in 2012 and 2013, respectively, whereas the 2011 displacement was

Table 1 Displacements (mm/year) detected by extensometers

Year	EXT4	EXT5	EXT6
2011	3.3	0	0
2012	9.1	0	0
2013	12.5	0	0

3.3 mm/year only). These results can be interpreted on the basis of the available information about the morphological and geomechanical configuration of the rock mass. The joint monitored by EXT4 is open and active, whereas the other monitored joints are not affected by displacements.

The monitoring system is completed by two piezoelectric transducers (PZTs), with frequency band 20–30 kHz, operating since January 2011. Each PZT is coupled to a steel waveguide placed on a horizontal borehole (AEWG1 and AEWG2 in Fig. 2b).

3 Laser scanning

Terrestrial laser scanning (TLS) is often used to examine the conditions of instability of a rock cliff because it provides dense, homogeneous, detailed and accurate 3D data of a slope surface, acquired in a remote and safe way. For 100 m acquisition distances, the precision can be ∼1 cm and, similarly, the spatial resolution can reach 1 cm (i.e., ∼1/3 of the laser spot diameter) if an adequate sampling step is used (Pesci et al. 2011). Aerial laser scanning (ALS) provides high-resolution topographic data over wide areas, with typical sampling steps of 20–30 cm for flight altitudes in the range of 600–1,000 m above ground level, and 10 cm precision. Since TLS data are taken from the ground, the incidence of laser beam on vertical surfaces is near to the normal one, leading to a good geometrical modeling of sub-vertical cliffs. However, TLS-based descriptions of mountain summit areas, or of large flat areas, are generally poor. On the contrary, ALS provides good data for summits and flat areas, but it is unable to characterize sub-vertical cliffs. An integration of TLS and ALS data therefore provides a complete geometrical reconstruction of the observed slope at different scales, overcoming the limits of the two single acquisition systems (Viero et al. 2010).

The TLS survey was carried out in March 2011 by means of an Optech ILRIS 3D instrument (Optech 2014). In order to investigate the whole cliff, seven scans were taken from a single viewpoint (VP) (Fig. 1, VP 1), with different rotations and tilts of the instrument. The distance ranged from 60 (6.4 cm sampling step) to 120 m (12.8 cm sampling step). The vertical extension of the acquired region ranged from 710 to 840 m a.s.l. because this area best shows the geological setting of the rock mass. In particular, the fact that a scree slope covers the bottom part of the limestone cliff up to 710 m a.s.l. was taken into account.

The ALS data had been previously acquired by Friuli Venezia Giulia Region, in order to acquire a panoramic and sufficiently detailed view of the Passo della Morte area. An Optech ALTM 3033 instrument, mounted on a helicopter, was used. The survey consisted of five 600-m-wide strips, with 20 % overlapping between adjacent strips, in a North–South direction, with a mean helicopter speed of 135 km/h and a mean relative altitude of 1,300 m. The mean density of the complete point cloud was 5 pts/m^2.

An ALS-based 3D point cloud is reconstructed from the scattered points on the basis of the series of instantaneous position, attitude and velocity of the airplane/helicopter. The data provided by the on-board navigation systems are completed by data from a network of GPS static receivers on the ground. For these reason, ALS data are always georeferenced. In the case of the Passo della Morte landslide, the TLS data were georeferenced by means of their alignment to the ALS data in the overlapping areas. To do so, the ICP (iterative closest point) algorithm available in the PolyWorks software package (Innovmetric 2014) was used.

Figure 3a shows the digital elevation model (DEM) of the whole system (cliffs and valley), obtained by the fusion of TLS and ALS data, where the Tagliamento River and the path of the abandoned national road can be seen. The grid side is 2.5 m. The TLS data make it possible to generate a detailed 3D triangulated model that can be used for distance, surface and volume computation purposes. Figure 3b shows a digital model of the studied cliff, with mean triangle size of 7 cm, where some interesting measurements are reported.

The TLS-based geomechanical analysis provides interesting information about the discontinuity surfaces, in particular the orientation and clustering properties (Slob et al. 2005), and, therefore, aids the positioning of on-site measurement systems. Figure 4 shows the results of such an analysis. Four main families of discontinuities are recognized: the bedding plane, which separates the layers of the stratified rock mass and whose dip angle and azimuth are 73° and 170°, respectively (73/170), and the joint sets (JSs) 1, 2 and 3.
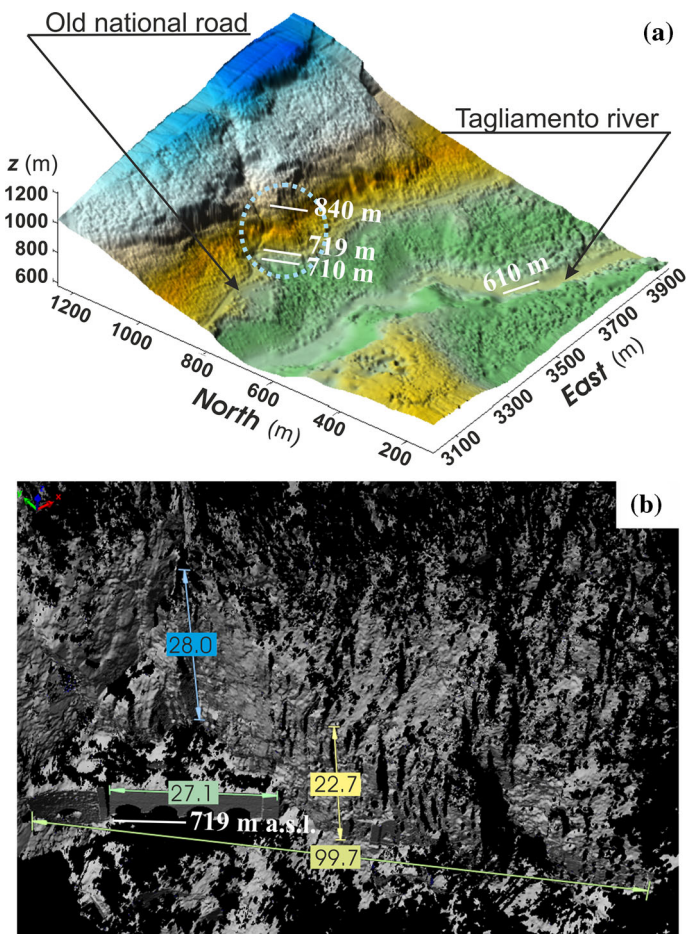
Fig. 3 Laser scanning models: **a** digital elevation model of area obtained from aerial laser scanning, where the west cliff of Passo della Morte landslide and some elevations are highlighted; **b** triangulated model of studied cliff, where some measures are shown. Positions of two sub-vertical discontinuity planes are also shown
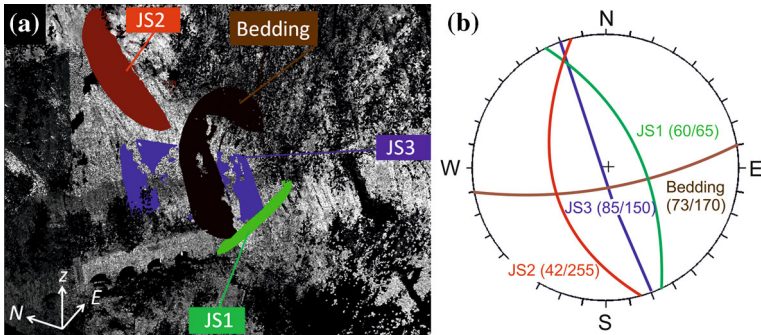
Fig. 4 Results of TLS-based geomechanical analysis: **a** some planes belonging to the detected discontinuity surfaces (a plane for each of the four families, i.e., bedding and JS1-JS3); **b** stereoplot of discontinuity orientations

4 Thermal imaging-based weakness recognition

4.1 Methods

A camera for IRT, or thermal imaging, is sensitive to distant infrared radiation (wavelength ≈ 0 μm) and therefore is able to acquire the thermal radiation pattern of a surface. The energy that reaches the pixel ij of a bolometer during the integration time is transformed into a temperature through a calibration procedure (Maldague 2001; Spampinato et al. 2011). The final result of an IRT measurement is a thermal image, i.e., a gray-level image with the information necessary to reconstruct the temperature matrix: temperature limits and laws connecting gray level and temperature.

IRT is currently used to recognize material weakness in a rock cliff (Wu et al. 2005; Teza et al. 2012). This is because shallow non-homogeneities of the material (e.g., a layer or an intrusion of a material inside the matrix of another material, shallow holes, moisture or fluid percolation, cracks or particularly fractured shallow zones) lead to differences in thermal transfer efficiency and therefore in radiated energy. IRT is a contactless technique, making for safe observational sessions and fast inspection rates. Nevertheless, no more than a shallow layer (some tens of centimeters) of a cliff can be studied by means of IRT.

Weakness recognition is carried out by evaluating the time history of the running, self-referenced thermal contrast (RTC) computed from each thermal image taken during a thermal transient, preferably a night cooling to have a reasonable noise level. The approach shown by Teza (2014), and the corresponding MATLAB implementation (THIMRAN toolbox), is used for the data analysis. Let $T_0, T_1, \ldots, T_N$ be $N + 1$ thermal images, registered on the same reference frame, taken at the times $t_0, t_1, \ldots, t_N$. The temperature related to the pixel ij at time t_k is $T_{ij}(t_k)$. In order to reduce possible fluctuations due to registration errors and/or thermal variability, it can be computed, for the pixel ij, the value $\langle T_{ij}(t_k) \rangle_{2n+1}$ averaged on the $(2n + 1)$-side square centered on this pixel ($n \in \mathbf{N}$). The RTC is defined by (Omar et al. 2005):

$$\mathrm{RTC}_{ij}(t_k) = \langle T_{ij}(t_k) \rangle_{2n+1} - T_{mn,ij}(t_k), \tag{1}$$

where $m > n$ and $T_{mn,ij}(t_k)$ is the mean temperature in the square-frame-shaped neighborhood that surrounds this pixel and whose internal and external sides are $2n + 1$ and

$2m + 1$ pixels, respectively. According to Omar et al. (2005), a possible weakness threshold for the pixel ij is

$$|\text{RTC}_{ij}(t_k)| \geq \eta\, \sigma_{mn,ij}(t_k), \tag{2}$$

where $\sigma_{mn,ij}(t_k)$ is the standard deviation of temperature whose mean is $T_{mn,ij}(t_k)$ and η tunes the sensitivity of the weakness recognition process. The coefficient η should be chosen taking into account the signal-to-noise ratio (SNR). If the typical size of the expected features related to the weakness is l, the integer m should be such that $(2m + 1)p > l$, where p is the mean pixel size on the observed surface. However, in order to reduce the effects of possible non-uniform heating or cooling, the integer m should not be too large. According to Teza (2014), a pixel ij can be considered to be affected by weakness if the threshold (2) is exceeded in this pixel in at least 75 % of the thermal images taken during a complete thermal transient. Therefore, damage recognition is carried out on the basis of RTC time history.

4.2 Surveys

The method was applied to the west part of the Passo della Morte landslide. Four (i–iv) surveys were carried out, as summarized in Table 1. A FLIR T620 instrument (FLIR 2014a) was used. Data calibration was performed on the basis of material emissivity, acquisition distance and air temperature by means of FLIR QuickReport freeware (FLIR 2014b). After the data calibration, the thermal images were created in ASCII format so they could be analyzed with the THIMRAN MATLAB toolbox.

Three surveys were carried out during night cooling and provided valid results. The data obtained during day heating, survey (iii), were not good because partial cloud cover prevented an adequate heating of the cliff. Moreover, the information provided by survey (ii) was included in survey (iv). Therefore, the results of survey (iv), relating to the lower part of both zone A and zone B, and survey (i), relating to zone A only, are described here, in this order.

Survey (iv) focused on the lower part of the investigated rock cliff (Fig. 5a). The camera was positioned at a distance ranging from 60 to 100 m (the maximum distance in the right part of the wall), with spatial resolution ranging from 4 to 6.8 cm (Fig. 1, VP 2). The extension of the acquired area was 65 m × 18 m (elevation from 720 to 738 m a.s.l.). Figure 5b shows, for each pixel, the fraction of thermal images taken during the night cooling where the RTC is beyond the threshold (2), and Fig. 5c shows the results of the weakness recognition based on RTC computation by assuming $\eta = 0.8$ and $m = 7$. The choice of η came from a trial-and-error approach. The value of m, which implied a running square reference neighborhood with a 60 and 102 cm side at the 60 and 100 m distance, respectively, was chosen as a compromise solution between two opposing requirements: (a) The joint separation can range from a few to ten cm, with features duly recognized as having such sizes, and (b) the analysis should be local to avoid different heating/cooling effects. The pixels where the RTC exceeds the threshold expressed by Eq. (2) in at least 75 % of the acquired thermal images are the red ones in Fig. 5c. Some points are selected to show the behavior of RTC time histories in both suspected weakness features and rock assumed to be sound. The corresponding RTC time histories are shown in Fig. 5d, where it can be noted that the RTC trend rapidly converges to 0 in the sound rock. A potential open joint can be easily recognized (point 1). The data provided by EXT4 confirm that this element is actually an open joint. Point 2 belongs to an interesting joint. Although it does
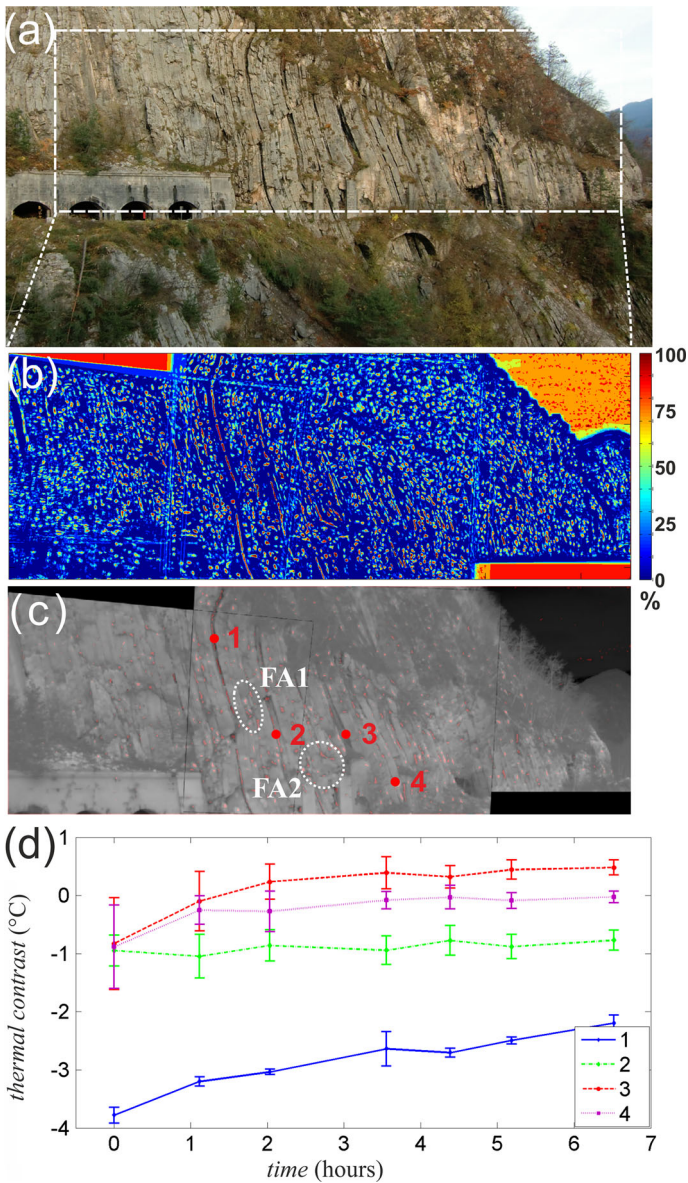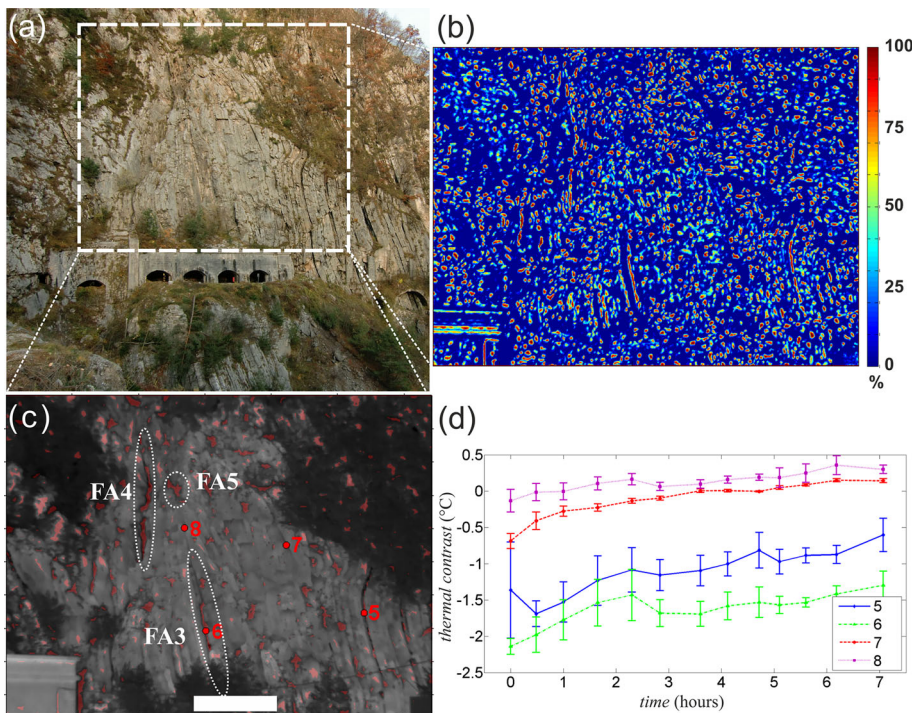
Fig. 5 Lower part of Passo della Morte west cliff (zones A and B): **a** visual image; **b** map of fraction of thermal images whose RTC is beyond the threshold; **c** results of IRT-based weakness recognition carried out on a mosaic of thermal images, where some selected points are highlighted (*1–4*) together with some examples of false positive due to vegetation cover (FA1 and FA2); and **d** running thermal contrast time history for the points highlighted in (**c**)

not seem at present to be an open joint, the fact that the pixels over the threshold are aligned and cover about 50 % of its persistence requires caution and suggests future analyses. The IRT-based analysis does not show other potential open joints. This is very

important because the extensometers EXT5 and EXT6 do not show deformations. The fact that for some pixels the RTC is over the threshold level is related to vegetation cover (elements FA1 and FA2 in Fig. 5c). These false alarms can be easily removed by comparison between the results of IRT analysis and color images (vegetation cover) and the TLS-based digital model (morphology/observational combination). It should be noted that the recognized open and partially open joints belong to zone B (Fig. 2b).

Survey (i) focused on the eastern part of the rock cliff, i.e., zone A mentioned in Sect. 2.1 above (Fig. 6a). In order to investigate a relatively large area (extension 45 m × 35 m, elevation from 724 to 759 m a.s.l.), the measurements were taken from the same position where the TLS was placed (Fig. 1, VP 1). Therefore, the mean acquisition distance was 110 m, with a mean spatial resolution of 8 cm. Figure 6c shows the results of the weakness recognition based on RTC computation by assuming $\eta = 0.8$ and $m = 7$ like the case of the previously described survey (iv). No significant signals of rock weakness appear in zone A, according to the known geological setting. Point 6 belongs to a linear element with RTC over the threshold level, but this is a false alarm because the local area is partially shaded from the sun, thus creating anomalous cooling compared with the surrounding area, FA3. However, such a false alarm can be easily removed by cross-validation with TLS data. The cross-validation can be manually performed by means of simultaneous inspection of TLS-based point cloud and RTC map. Other false alarms exist,

Fig. 6 Upper left part of Passo della Morte west cliff (zone A): **a** visual image; **b** map of fraction of thermal images whose RTC is beyond the threshold; **c** results of IRT-based weakness recognition, where some selected points are highlighted (5–8) together with some examples of false positive due to morphology (FA3) and vegetation cover (FA4 and FA5); and (**d**) running thermal contrast time history for points highlighted in (**b**)

but they can be easily recognized as due to vegetation cover, as in the case of survey (iv). In the right part of the investigated area, the previously recognized open joint can be seen; point 5 in Fig. 6c corresponds to point 1 in Fig. 5c.

5 Results and discussion

A reliable evaluation of the spatial position of each joint and the joint spacing, separation, persistence and roughness are required for a meaningful assessment of rockfall-induced hazard. The data provided by TLS can be used for both a geometrical and geomechanical investigation of a rock mass. In particular, TLS-based modeling of discontinuity surfaces pinpoints joint positions and spacing. Such modeling also provides information on joint separation and persistence, but this information is partial and is not enough for a complete picture of the joint's properties. As demonstrated above, IRT is able to fill this information gap, since the separation and persistence of joints can be obtained by means of analysis of the time history of thermal contrast during a thermal transient.

Both TLS and IRT are remote sensing techniques. Therefore, the measurements can be carried out quickly from positions where the rockfall hazard is either low or negligible. TLS-based data gathering of a whole cliff can be carried out in a day, and also the data analysis and modeling are not time consuming. Similarly, an IRT measurement session can be effected during a cooling night, and the data can also be quickly analyzed and weakness areas recognized. Moreover, if changes in damage/weakness of the rock slope are rapid, or are believed to be so, the measurement sessions can be easily repeated. Although the price of a TLS or an IRT instrument is relatively high, the cost of a single measurement session (or of a series of sessions) is low.

Since IRT provides 2D images, a correct interpretation of the thermal contrast maps requires a 3D model. As already stated, the coupling of local morphology and observational conditions can lead to features apparently above the thermal contrast threshold. A comparison between the thermal contrast map and the 3D digital model means these apparent features can be recognized (see, e.g., the digital model in Fig. 3b and the false alarm area FA3 shown in Fig. 6c). A TLS-based reference model can be generated once and for all as the monitoring program starts, and the thermal imaging sessions can be periodically carried out. If a cliff has a substantially 2D shape (e.g., absence of protruding blocks, folds or other intrinsically 3D features), a reasonable IRT-based description of the joints might render superfluous the use of TLS data. Equally, in some cases, the joints are so opened that an IRT-based examination might be unnecessary. However, the typical shape and geostructural layout of a rock cliff require an integrated use of TLS and IRT for an adequate joint characterization. The IRT-based weakness area recognition was performed by analyzing the time history of the running, self-referenced thermal contrast (RTC), where the thermal contrast was computed for each pixel with respect to a neighboring reference square area. Alternatively, the absolute thermal contrast (ATC), computed with respect to a reference area characterized by known sound rock, could be adopted (Maldague 2001). The ATC was successfully used by Teza et al. (2012) in two test sites and was also used to analyze the dataset of survey (i) (Table 2), in the Passo della Morte site. The results show that the ATC-based weakness area recognition provided the same results as the RTC-based one. Nevertheless, the use of RTC is recommended because its sensitivity to non-homogeneous heating/cooling and vegetation cover-induced noise is lower than ATC's.

Table 2 Details about IRT measurement sessions, including mean acquisition distance and resolution

N°	Date	Camera position	Distance (m)	Resolution (cm)	Start	End	Duration	Taken images
(i)	June 29/30, 2012	VP1	100–120	6.8–8.0	23.05	6.10	7 h 4 min	13
(ii)	August 5/6, 2012	VP2	60–100	4.0–6.8	23.15	6.15	7 h	11
(iii)	April 22, 2013	VP2	60–100	4.0–6.8	11.18	17.15	5 h 67 min	6
(iv)	April 26/27, 2013	VP2	60–100	4.0–6.8	19.15	1.36	6 h 21 min	6

As expected, all the observations carried out during the evening/night cooling provided good quality data for reliable weakness area recognition based on analysis of the time history of RTC. However, the observation carried out during the day heating (late morning and afternoon because the cliff faces SSW) was unable to provide useful results because an adequate temperature difference was not reached on a cloudy day. The conclusions are that a measurement session must cover the main part of a thermal transient with an adequate temperature difference and that, in an Alpine area, it should be carried out in late spring, summer and early autumn.

The data provided by extensometers placed on the rock mass validate the results of the IRT measurements. According to extensometer measurements, the joint with thermal contrast above the thresholds throughout the thermal transients and with significant persistence belongs to an unstable area. IRT measurements suggest it is an open joint, and the data gathered by extensometers confirm this. On the contrary, where the extensometers do not record significant displacements, the thermal contrast is always below the threshold or exceeds the threshold in the first stages of the transient only. The corresponding joint characters are therefore well detected. In general, the deformation data and the IRT data are in agreement.

These results suggest an operational strategy in the management of rockfall-induced hazard assessment and monitoring. If a new weakened and perhaps collapse-prone area is recognized, signaled, for example, by fallen blocks or noise coming from the mass as an effect of rock fracturing and/or motion, TLS and IRT can provide speedy preliminary data to give a reliable picture of the geostructural characteristics of the unstable mass. In this way, it is possible to recognize those areas that should be studied more in detail with on-site techniques like conventional geomechanical scan-line, extensometers, AT/MT sensors and so on. Attenuation of MTs and, especially, of AEs is so high that the sensors cannot be placed more than a few meters distant from their source, e.g., rupture of a rock bridge in an open joint (Schenato et al., 2013). The arrangement of MT/AE sensors can be strongly aided by the results of TLS and IRT measurements. IRT can be used for this purpose because an observation of the cliff throughout a thermal transient (in particular, a night cooling) makes it possible a fast and low-risk recognition of areas characterized by anomalous thermal transfer, in particular open joints. The repetition of IRT observations allows a recognition of possible changes of the rock mass kinematics and geostructural setting. As slope instability increases, other weakness areas could appear because a fair joint could change into an open joint, which would then require monitoring with extensometers or other instruments. Moreover, the results of the IRT analyses highlight the presence of a joint which at present is fair, but with a significant proportion of pixels above the threshold level. This suggests that further changes to this joint could occur and, therefore, that future IRT surveys are recommended. In general, the integrated use of TLS and IRT reliably recognizes those joints where extensometers or other monitoring sensors

should be placed. It can be considered a preparatory activity toward a landslide hazard assessment, which can also discriminate between the weakened areas and the solid ones. Clearly, TLS and IRT cannot directly provide a hazard zonation, but their integration can be a significant part of a hazard assessment procedure.

The data obtained by the surveys so far carried out can be used for a hazard zonation on the basis of the density of active discontinuity surfaces and, if completed by numerical modeling, can make it possible to formulate hypotheses about the magnitude of expected instability phenomena. The results make it possible to independently position the border between zone A and zone B, where the latter is characterized by a higher rockfall hazard. In particular, the joint recognized as active (Figs. 5c, 6c) can be assumed to be such a border and currently is the most important feature of zone B, since possible sliding there can be considered the most probable cause of a significant rock collapse in the Passo della Morte area. For this reason, the most probable evolutionary scenario is a failure with a moving volume of 450,000 m^3.

6 Conclusions

The experiences matured in the Passo della Morte test site show that the integrated use of TLS and IRT provides significant information about the geometry and kinematics of a sedimentary rock mass with sub-vertical discontinuity planes. Besides the evaluation of the discontinuity surface orientations and other geometric information, the recognition of the open joints and therefore of the discontinuities that could turn into sliding surfaces is feasible.

The results so far achieved agree very well with those provided by extensometers. This implies that TLS and IRT, which are contactless techniques able to perform fast, easy and relatively low-cost surveys, can be used to recognize the areas where on-site conventional and expensive detectors like extensometers, inclinometers and AE sensors should be placed to effect good real-time monitoring of a rock mass that had never been previously studied. The repetition of IRT surveys can even provide information about the evolution of the joints. In particular, joints, which are fair in a preliminary survey, could change with time and IRT is able to recognize this, suggesting the improvement of already installed monitoring systems.

Moreover, TLS and IRT provide information that can be directly used for rockfall hazard assessment. These techniques are unable to perform real-time monitoring, but information about mass movements is very important for the detection of elements where detachment is imminent.

References

Arosio D, Longoni L, Papini M, Scaioni M, Zanzi L, Alba M (2009) Towards rockfall forecasting through observing deformations and listening to microseismic emissions. Nat Hazards Earth Syst Sci 9(4):1119–1131

Budetta P (2010) Application of the Swiss Federal Guidelines on rock fall hazard: a case study in the Cilento region (Southern Italy). Landslides 8(3):381–389

Cai M, Morioka H, Kaiser P, Tasaka Y, Kurose H, Minami M, Maejima T (2007) Back-analysis of rock mass strength parameters using AE monitoring data. Int J Rock Mech Min Sci 44(4):538–549

Codeglia D (2011) Analisi geomeccanica e predisposizione di un sistema di monitoraggio lungo la galleria del Passo della Morte. Master's Degree Thesis, Trieste University (in Italian)

Corominas J, Moya J, Lloreta A, Gili JA, Angeli MG, Pasuto A, Silvano S (2000) Measurement of landslide displacements using a wire extensometer. Eng Geol 55(3):149–166

Corominas J, Copons R, Moya J, Vilaplana JM, Altimir J, Amigó J (2005) Quantitative assessment of the residual risk in a rockfall protected area. Landslides 2(4):343–357

Deparis J, Garambois S, Hantz D (2007) On the potential of Ground Penetrating Radar to help rock fall hazard assessment: a case study of a limestone slab, Gorges de la Bourne (French Alps). Eng Geol 94(1–2):89–102

Dixon N, Spriggs M (2007) Quantification of slope displacement rates using acoustic emission monitoring. Can Geotech J 44(6):966–976

Dixon N, Spriggs M, Marcato G, Pasuto A (2012) Landslide hazard evaluation by means of several monitoring techniques, including an acoustic emission sensor. In: Eberhardt E, Froese C, Turner K, Leroueil S (eds) Landslides and engineered slopes. CRC Press, London, pp 1405–1411

FLIR (2014a) FLIR ThermaCAM T620 technical datasheet. http://www.flir.com/cs/emea/en/view/?id=41437. Accessed 24 Nov 2014

FLIR (2014b) FLIR QuickReport freeware download page. http://www.flir.com/thermography/eurasia/en/content/?id=11368. Accessed 24 Nov 2014

Franceschi M, Teza G, Preto N, Pesci A, Galgaro A, Girardi S (2009) Discrimination between marls and limestones using intensity data from terrestrial laser scanner. ISPRS J Photogramm Remote Sens 64(6):522–528

Hack R (2000) Geophysics for slope stability. Surv Geophys 21:423–448

Innovmetric (2014) Innovmetric PolyWorks software description. http://www.innovmetric.com/polyworks/3D-scanners/home.aspx. Accessed 24 Nov 2014

Maldague X (2001) Nondestructive evaluation of materials by infrared thermography. John Wiley, Chichester

Marcato G (2007) Valutazione della pericolosità da frana in località Passo della Morte (UD) (Evaluation of landslide hazard in Passo della Morte, Udine). PhD Dissertation, Modena and Reggio Emilia University (in Italian)

Monegato G, Vezzoli G (2011) Post-Messinian drainage changes triggered by tectonic and climatic events (Eastern Southern Alps, Italy). Sedim Geol 239:188–198

OGS (2014) The Friuli Venezia Giulia seismometric network home page. http://www.crs.inogs.it/bollettino/RSFVG/RSFVG.en.html. Accessed 24 Nov 2014

Omar M, Hassan MI, Saito K, Alloo R (2005) IR self-referencing thermography for detection of in-depth defects. Infrared Phys Technol 46(4):283–289

Oppikofer T, Jaboyedoff M, Blikra L, Derron M (2009) Characterization and monitoring of the Åknes rockslide using terrestrial laser scanning. Nat Haz Earth Syst Sci 9:1003–1019

Optech (2014) Optech ILRIS-3D technical data. http://www.optech.com/index.php/product/optech-ilris-scan/. Accessed 24 Nov 2014

Pesci A, Teza G, Bonali E (2011) Terrestrial laser scanner resolution: numerical simulations and experiments on spatial sampling optimization. Remote Sens 3(1):167–184

Pisa G (1972) Tentativo di ricostruzione paleoambientale e paleostrutturale dei depositi di piattaforma carbonatica medio-triassica delle Alpi Carniche sud-occidentali. Mem Soc Geol It 13:35–83 in Italian

Schenato L, Palmieri L, Autizi E, Calzavara F, Vianello L, Teza G, Marcato G, Sassi R, Pasuto A, Galgaro A, Galtarossa A (2013) Rockfall precursor detection based on rock fracturing monitoring by means of optical fibre sensors. Int J Sust Mater Struct Sys 1(2):123–141

Singhroy V, Molch K (2004) Characterizing and monitoring rockslides from SAR techniques. Adv Space Res 33(3):290–295

Slob S, van Knapen B, Hack R, Turner K, Kemeny J (2005) A method for automated discontinuity analysis of rock slopes. Transport Res Rec 1913(1):187–208

Spampinato L, Calvari S, Oppenheimer C, Boschi E (2011) Volcano surveillance using infrared cameras. Earth-Sci Rev 106:63–91

Sturzenegger M, Stead D (2009) Close-range terrestrial digital photogrammetry and terrestrial laser scanning for discontinuity characterization on rock cuts. Eng Geol 106(3–4):163–182

Teza G (2014) THIMRAN: a MATLAB toolbox for thermal image processing aimed at damage recognition in large bodies. J Comput Civil Eng 28(4, 04014017):1–8

Teza G, Pesci A, Genevois R, Galgaro A (2008) Characterization of landslide ground surface kinematics from terrestrial laser scanning and strain field computation. Geomorphology 97(3–4):424–437

Teza G, Marcato G, Castelli E, Galgaro A (2012) IRTROCK: a MATLAB toolbox for contactless recognition of surface and shallow weakness of a rock cliff by infrared thermography. Comput Geosci 45:109–118

Viero A, Teza G, Massironi M, Jaboyedoff M, Galgaro A (2010) Laser scanning based recognition of rotational movements on a deep seated gravitational instability: the Cinque Torri case (North-Eastern Italian Alps). Geomorphology 122:191–204

Walter M, Schwaderer U, Joswig M (2012) Seismic monitoring of precursory fracture signals from a destructive rockfall in the Vorarlberg Alps, Austria. Nat Hazards Earth Sys Sci 12(11):3545–3555

Wu JH, Lin HM, Lee DH, Fang SC (2005) Integrity assessment of rock mass behind the shotcreted slope using thermography. Eng Geol 80(1–2):164–173